Paper No.
16570

CORROSION 2021 Virtual Conference & Expo April 19-30

AMPP Association for Materials Protection & Performance

Evaluating the Corrosion Performance of Materials in Solar Nitrate Salts

Keenan O'Neill[1], John Groth[2], Helena Alves[3], and Dev Chidambaram[1,*]

[1]Materials Science and Engineering, University of Nevada, Reno, Reno, NV 89557-0388.

[2]VDM Metals USA, Reno, NV 89506

[3]VDM Metals International GmbH, Plettenberger Str. 2, Werdohl, Germany

*dcc@unr.edu

Abstract

The corrosion behavior of two alloy samples was analyzed using potentiodynamic polarization in a molten nitrate medium at 500°C. The Tafel region of the polarization curves was extrapolated to calculate the exchange current density and corrosion potential. Gravimetric analysis was also conducted to determine the mass change due to corrosion. The performance of these alloys was approximated using these values to screen these materials for further testing in this environment. The exchange current density was lowest for UNS N06230 at 0.233mA/cm^2 and highest for UNS N06625 GR1 at 0.389mA/cm^2.

Key words: Molten solar salts, $NaNO_3$, KNO_3, Potentiodynamic, Nickel alloys, VDM, Alloy 625

Introduction

Corrosion testing is a necessary step in the materials design and selection process for any application. Costs associated with corrosion made up 3.1% of the United States' total GDP in 1998 and it is reported that this percentage has stayed the same up until 2003.[1] Corrosion testing is exceedingly important in environments where materials will be subjected to high temperatures as

high temperatures and the presence of oxygen generally cause pure metals to be oxidized. Some oxide layers can be protective but the influence of ions in the environment can break down these oxide layers. Molten salts are a very corrosive environment due to the high concentration of ions present and the high temperatures associated with their uses. One specific application for molten salt is in concentrated solar power (CSP) which uses parabolic mirrors to direct sunlight onto a central point. This is generally a reservoir of some heat transfer fluid, such as a molten nitrate salt blend, where the reservoir material must have excellent resistance to corrosion. In addition to the reservoir at the heating point, most systems incorporate a thermal energy storage reservoir to store heated molten salt to continuously generate energy. Therefore, the corrosion resistance of the reservoir materials is of the utmost importance for this form of power. Multiple studies have been conducted on the corrosion behavior of different alloys in molten nitrate salts with varying results.[2–8] The general practice for observing the corrosion behavior of a material is to conduct a long-term exposure of the material in the salt as was the case in many of the cited studies. These tests are generally very long ranging from 50 hours to thousands of hours and require constant heating for the duration. This can become costly in terms of both electrical costs and labor costs as the experimental setup needs to be monitored periodically throughout the duration.

Electrochemically accelerated corrosion is a type of testing that utilizes an applied voltage or current to accelerate corrosion of the samples. Potentiodynamic polarization testing applies a range of voltages and measures the resulting current to generate a polarization curve which can then be used to approximate the exchange current density and corrosion potential.[6,9] This significantly

reduces the time required for testing of a given material allowing studies to require less time for testing and reduced electrical costs. However, having a significantly shorter exposure time also means that oxide films have significantly less time to form and may not fully develop into a protective layer. Specific forms of corrosion such as pitting, selective leaching, and intergranular corrosion may also not be observed in the samples as there is not adequate time for these processes to occur. The short time under exposure is ideal for observing the initial steps of corrosion occurring on the samples. Therefore, the use of electrochemically accelerated corrosion testing should be used to screen materials for additional testing to avoid unnecessarily testing a poorly performing sample for the long duration required for exposure testing. In this study, two alloy samples were screened using potentiodynamic polarization testing to calculate the exchange current density and corrosion potential.

Experimental Procedure

The two samples were annealed UNS N06230 and annealed UNS N06625 GR1. The UNS N06625 GR1 sample was annealed at 1742 to 1922 ^{o}F and met the requirement for ASTM B443 Grade 1. The UNS N06230 sample was annealed at 2150 ^{o}F to 2275 ^{o}F. Both samples were tested in their as-received state with a final sanded surface preparation of 120 grit for consistency between samples. The composition in weight percent for each of the two samples is listed in Table 1. Prior to any experiments, the samples were cleaned with acetone followed by isopropanol and finished with deionized water. The samples were wiped dry post-rinsing to ensure no residue remained. The salts used in this study were sodium nitrate and potassium nitrate and both met or exceeded American Chemical Society purity standards. These salts were subjected to a drying process consisting of a 24-hour, open-air oven baking at 170°C before being bottled and stored in a

desiccant chamber. The off-eutectic mixture was 60wt% sodium nitrate and 40wt% potassium nitrate with an average total mass of 30g per test. The salt eutectic was placed in an alumina crucible in a furnace set to 500℃ under air. A two-electrode setup was used for all experimentation with a UNS N06625 counter, platinum wire pseudo-reference, and sample working electrodes. Collection of the open circuit potential (OCP) was conducted for 1.25 hours prior to potentiodynamic polarization testing with a 5 mV/s scan rate between -0.5V and 1V against the OCP. The electrodes were allowed to cool in a desiccant chamber post-exposure and were rinsed with deionized water to remove any leftover salt residue after cooling. All electrochemical testing and data collection was done using a potentiostat with data analysis conducted using the manufacturer's software. The exposed area for the samples was measured using a standard ruler with an uncertainty of $\pm 0.25 mm^2$. Photographs were taken of the samples before and after exposure to display the appearance of the corrosion layer. Gravimetric analysis was conducted on the samples to determine the mass change post-testing.

Results and Discussion

The results for the polarization curves of each alloy sample are given in Figure 1. The corrosion potential (E_{corr}) and exchange current density (i_{corr}) were calculated from the intersection of the extrapolated Tafel regions of the cathodic and anodic sections of the polarization curves. The Tafel region was approximated to be the region of the graph with the most constant slope. Gravimetric analysis for the samples was inconclusive due to the low magnitude of mass change observed. Photographs of the samples were taken before and after exposure to the molten salt and are shown in Figure 2. The photographs of the samples illustrate the difference between pre- and post-exposure samples as well as the difference in vapor-phase and liquid-phase corrosion.

The areas on the polarization curve with the most constant slope are known as the Tafel regions and are present on both the anodic and cathodic sections of the curve. The data collection was not modified with an area as no legitimate measurement of exposed area could be conducted prior to testing. Therefore, all current values recorded by the potentiostat were divided by the total exposed area to yield current density for all given polarization curves. Linear extrapolation of the Tafel regions on a semi-logarithmic plot yields the exchange current density and corrosion potential at the intersection of these lines. Through this process, an approximation of the exchange current density and corrosion potential for the alloy samples were identified. The values for the tested samples are given in Table 2 along with values for other alloys obtained from literature.[6,9] The recorded values for the exchange current density are not direct representations of how a material will perform in a given environment due to the short exposure time. These values are only representative of how a base metal would behave without considering the effect of oxide formation, pitting behavior, or the effect of selective leaching and intergranular corrosion. Due to this, the values for the exchange current density for a sample more resistant in a given environment may be lower than a sample less resistant. The highest calculated exchange current density of the two samples was for UNS N06625 GR1 at 0.389mA/cm^2. This was higher than the calculated value of SS 316 given in a separate study.[9] However, it has been reported in literature that UNS N06625 has significantly less corrosion in the solar salt blend than SS 316 due to the formation of a sparsely porous oxide layer.[10] The thickness of the scale formation on SS 316 was significantly thicker than UNS N06625 which also indicates that this oxide layer was not protective. This conclusion is corroborated by other research on stainless steel in this salt that observes selective leaching of chromium.[2,4,10] The exchange current density presented in this study only accounts for

the raw corrosion resistance of the sample at the time of exposure. Generally, these samples have not yet developed any form of oxide layer which could protect the samples from corrosion. The exposure time is also inadequate to observe types of corrosion such as pitting or intergranular corrosion. Selective leaching of specific elements in the samples may be observed through surface analysis with precise scans targeting the uppermost layer of the samples. The exchange current density for UNS N06230 was the lowest at 0.233 mA/cm^2. It has been reported that tungsten oxide dissolves in potassium nitrate into a tungstate ion (WO_4^{2-}) which may be the mechanism of corrosion of UNS N06230 in this study.[11] There is a high concentration of tungsten in UNS N06230 but the same study reported that UNS N06230 forms a nickel oxide layer and undergoes uniform corrosion in this salt medium. The uniform corrosion reported for UNS N06230 is likely why the exchange current density for this sample was lower. This alloy is reported to perform better than some stainless steels but worse than UNS N06625 in this medium at this temperature.[12]

The shape of the polarization curve often yields insight into the underlying mechanisms of corrosion occurring in the tested samples. The curve for UNS N06230 indicated corrosion resistance to the solar salt medium as it had a portion where the slope was very steep indicating low changes in current density versus the voltage. This indicates that UNS N06230 is stable at a range of potentials in this medium. The polarization curve for UNS N06625 GR1 had a brief portion of the anodic curve with a negative slope. This region may indicate pseudo-passivity in the sample caused by the formation of a protective oxide layer. UNS N06625 is reported to form a protective oxide film in this medium which is indicated by this region of pseudo-passivity.[8,10,13] Due to the short time of exposure, the oxide film was likely not stable enough to fully passivate the sample. The polarization curve for UNS N06625 GR1 appears to have three distinct sections

on the anodic part. A similar result was seen in a study on the polarization curve of UNS N06625.[8] The study reported that the initial portion of the polarization curve was the formation of a nickel oxide film, followed by depletion of oxygen ions and dissolution of the film for the other two segments of the polarization curve.[8]

Conclusions

The two samples – UNS N06230 and UNS N06625 GR1 – underwent potentiodynamic polarization in a 3:2 mixture of molten sodium nitrate and potassium nitrate, respectively. The resulting polarization curves were analyzed and the Tafel regions were extrapolated to calculate the exchange current density and corrosion potential for the samples. The lowest exchange current density was 0.233mA/cm^2 for UNS N06230 with a corrosion potential of -237mV. The exchange current density for UNS N06625 GR1 was 0.389mA/cm^2 with a corrosion potential of -133mV. These samples both had higher exchange current densities than SS 316 as reported in literature due to the absence of a protective oxide layer that forms on these samples during long-term exposures in this medium. The polarization curve for UNS N06230 indicated corrosion resistance in the medium with no evidence of passivity. The polarization curve for UNS N06625 GR1 had a small region indicative of pseudo-passivity as referenced in research. The samples both performed well enough to be evaluated with long-term exposure studies to further understand the corrosion mechanisms.

Acknowledgements:

This work was funded in part by VDM Metals USA. Additional funding for this work was provided by Materials Characterization Nevada at the University of Nevada, Reno.

References

1. Koch, G. H., Brongers, M. P. H., Thompson, N. G., Virmani, Y. P., Payer, J. H. Corrosion costs and preventive strategies in the United States. *NACE International Report.* 1–12 (2002) doi:FHWA-RD-01-156.
2. Goods, S. H. & Bradshaw, R. W. Corrosion of Stainless Steels and Carbon Steel by Molten Mixtures of Commercial Nitrate Salts. *J. Mater. Eng. Perform.* **13**, 78–87 (2004).
3. Tortorelli, P. F., Bishop, P. S. & DiStefano, J. R. Selection of Corrosion-Resistant Materials for Use in Molten Nitrate Salts. 62 (1989).
4. Wang, W., Guan, B., Li, X., Lu, J. & Ding, J. Corrosion behavior and mechanism of austenitic stainless steels in a new quaternary molten salt for concentrating solar power. *Sol. Energy Mater. Sol. Cells* **194**, 36–46 (2019).
5. Soleimani Dorcheh, A. & Galetz, M. C. Slurry aluminizing: A solution for molten nitrate salt corrosion in concentrated solar power plants. *Sol. Energy Mater. Sol. Cells* **146**, 8–15 (2016).
6. Baljier, R., Yevtushenko, O. & Hattendorf, H. Suitability of high alloyed materials in molten salts at 600 °C. *NACE - Int. Corros. Conf. Ser.* **3**, 1812–1820 (2016).
7. Fernández, A. G. *et al.* Corrosion of alumina-forming austenitic steel in molten nitrate salts by gravimetric analysis and impedance spectroscopy. *Mater. Corros.* **65**, 267–275 (2014).
8. Khorsand, S., Sheikhi, A., Raeissi, K. & Golozar, M. A. Hot Corrosion Behavior of Inconel 625 Superalloy in Eutectic Molten Nitrate Salts. *Oxid. Met.* **90**, 169–186 (2018).
9. Summers, K. L. & Chidambaram, D. Corrosion behavior of structural materials for potential use in nitrate salts based solar thermal power plants. *J. Electrochem. Soc.* **164**, H5357–H5363 (2017).
10. Soleimani Dorcheh, A., Durham, R. N. & Galetz, M. C. Corrosion behavior of stainless and low-chromium steels and IN625 in molten nitrate salts at 600 °c. *Sol. Energy Mater. Sol. Cells* **144**, 109–116 (2016).
11. Kruizenga, A. M., Gill, D. D. & Laford, M. Materials Corrosion of High Temperature Alloys Immersed in 600 ° C Binary Nitrate Salt. *Sandia Rep.* (2013).
12. Kruizenga, A. M., Gill, D. D., Laford, M. & Mcconohy, G. Corrosion of High Temperature Alloys in Solar Salt at 400 , 500 , and 680 ° C. *Sandia Rep.* 1–45 (2013).
13. McConohy, G. & Kruizenga, A. Molten nitrate salts at 600 and 680°C: Thermophysical property changes and corrosion of high-temperature nickel alloys. *Sol. Energy* **103**, 242–252 (2014).

Figures and Tables

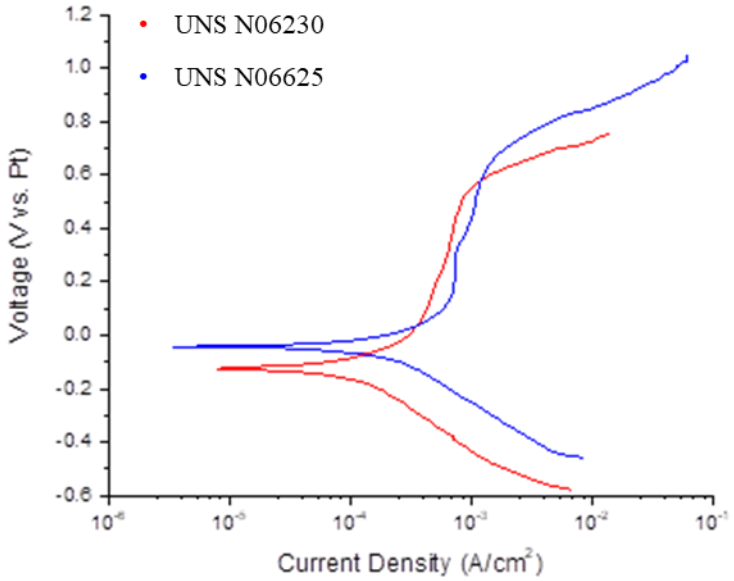

Figure 1: The polarization curves for UNS N06230 and UNS N06625 GR1, obtained at a scan rate of 5mV/s, indicate similar corrosion resistance but different behavior in the solar salt medium.

Figure 2: The alloy samples are shown after and before testing from left to right with UNS N06230 above and UNS N06625GR1 below.

Table 1: The chemical composition of the two samples is given in weight percent.

Element (wt%)	UNS N06230	UNS N06625 GR1
Ni	REM	61.17
Mo	1.24	8.5
W	13.90	-
Co	0.18	0.03
Al	0.41	0.10
Ti	<0.01	0.20
Cu	0.04	0.01
C	0.100	0.022
Cr	21.86	21.6
Fe	1.59	4.7
P	0.005	0.004
Mn	0.48	0.05
Si	0.34	0.19
S	<0.002	<0.001
B	0.003	-
La	0.017	-
Nb	-	3.32
Ta	-	0.01

Table 2: The values for the exchange current density (i_{corr}) and corrosion potential (E_{corr}) are given for the tested samples and samples tested in literature.

Alloy	i_{corr}(mA/cm^2)	E_{corr}(mV)
UNS N06230	0.233	-237.0
UNS N06625 GR1	0.389	-133.0
Stainless Steel 316[9]	0.183	-62.8
UNS N08810[9]	0.517	-59.1
UNS G41300[9]	0.321	-135.0
NiCr25FeAlYB[6]	~2.000	~-25.0